Proceedings of the Institute of Acoustics

PROPAGATION-INVARIANT CLASSIFICATION OF SHALLOW WATER SONAR SIGNALS [1]

Greg Okopal University of Pittsburgh, 348 Benedum Hall, Pittsburgh, PA 15261, USA
Patrick Loughlin University of Pittsburgh, 348 Benedum Hall, Pittsburgh, PA 15261, USA

1 INTRODUCTION

In active sonar, detection and classification of objects by their backscattered sonar signatures can be complicated by propagation effects. For example, sound waves propagating in sea water undergo frequency-dependent attenuation, as do sound waves penetrating the bottom sediment. The channel may also induce dispersion, which can be especially significant in shallow water channels, whereby different frequencies propagate at different velocities, resulting in temporal and spatial spreading of the wave [11, 13]. These propagation effects can cause the wave to change dramatically as it propagates. Accordingly, in such environments, different signatures do not necessarily reflect different objects/targets of interest, which can adversely impact automatic classification.

Our aim in this paper is to consider propagation-invariant classification, and in particular the extraction of features from the backscattered wave that are invariant to particular channel effects. We present a feature extraction process to obtain moment-like features of the wave that are invariant, per mode, to dispersion and exponential or power-law damping. Environmental knowledge is not needed, beyond knowing the general form of the damping, which is usually media-dependent and hence typically known. Simulations of classification of steel shells in channels with dispersion and damping demonstrate the utility of these features. The features are also robust against random variations in sound speed and damping.

2 BACKGROUND

2.1 Linear wave propagation

We give here a brief background on the normal mode solution for linear wave propagation [11, 13]. We also review ordinary moments, and our previously developed dispersion-invariant moment features [1, 5, 8]. In the following section, we then consider moment features that are invariant to both dispersion and damping.

Given an initial wave $u(0,t)$ generated at position $x = 0$, the propagated wave is given by [11, 13]

$$u(x,t) = \frac{1}{\sqrt{2\pi}} \int F(0,\omega)\, e^{jK(\omega)x}\, e^{-j\omega t}\, d\omega = \frac{1}{\sqrt{2\pi}} \int F(x,\omega)\, e^{-j\omega t}\, d\omega \tag{1}$$

per mode, where $K(\omega)$ is the dispersion relation expressed in terms of wavenumber k as a function of radial frequency ω and $F(0,\omega)$ is the spectrum of the initial pulse,

$$F(0,\omega) = \frac{1}{\sqrt{2\pi}} \int u(0,t)\, e^{j\omega t}\, dt \tag{2}$$

[1] Work supported by the Office of Naval Research (N000140710355 and N000140610009).

(For simplicity, we consider a single spatial dimension x, which denotes range.) The dispersion relation can be either purely real or complex. If the dispersion relation is complex, then there is damping, resulting in frequency-dependent attenuation as the wave propagates. Propagation without dispersion or damping is characterized by $K(\omega) = \omega/c$.

Writing the dispersion relation explicitly in terms of its real and imaginary parts,

$$K(\omega) = K_r(\omega) + j\, K_i(\omega) \tag{3}$$

and noting from (1) that $F(x,\omega) = F(0,\omega)e^{jK(\omega)x}$, it follows that the spectrum of the wave can be written in terms of amplitude and phase as

$$F(x,\omega) \;=\; B(x.\omega)e^{j\psi(x,\omega)} \tag{4}$$

where

$$B(x,\omega) \;=\; B(0,\omega)e^{-K_i(\omega)x} \tag{5}$$

$$\psi(x,\omega) \;=\; \psi(0,\omega) + K_r(\omega)x \tag{6}$$

and where $B(0,\omega)$ and $\psi(0,\omega)$ are the spectral amplitude and phase, respectively, of the initial wave $u(0,t)$.

2.2 Ordinary and Dispersion-Invariant Moments

If there is dispersion but no damping ($K_i(\omega) = 0$), then spectral moments may be useful features for classification, since they do not change, per mode, with propagation distance x:

$$\langle\omega^n\rangle_x \;=\; \int \omega^n |F(x,\omega)|^2 d\omega \;=\; \int \omega^n |F(0,\omega)|^2 d\omega \;=\; \langle\omega^n\rangle_0 \tag{7}$$

However, temporal moments, such as the duration of the wave, do change with propagation distance in a dispersive channel, and hence are not "propagation-invariant" features for classification.

Time-domain moment-like features that are invariant to dispersion can be defined; these are given by [5, 8]

$$A_n(x) \;=\; \int F^*(x,\omega) \left(j\frac{\partial}{\partial\omega} - t_g(x,\omega)\right)^n F(x,\omega)\, d\omega \tag{8}$$

where $t_g(x,\omega) = -\psi'(x,\omega)$ is the *group delay* of the wave. These moments are similar to central temporal moments,

$$\langle (t - \langle t\rangle_x)^n \rangle_x \;=\; \int u^*(x,t)\,(t - \langle t\rangle_x)^n\, u(x,t)\, dt \tag{9}$$

$$\;=\; \int F^*(x,\omega) \left(j\frac{\partial}{\partial\omega} - \langle t\rangle_x\right)^n F(x,\omega)\, d\omega \tag{10}$$

but with an important difference: rather than being centered about the average time $\langle t\rangle_x$, the "dispersion-invariant moments" defined by (8) are centered about the group delay $t_g(x,\omega)$ of the wave. This centering about the group delay renders these moments independent of x,[1, 5]

$$A_n(x) = A_n(0) \tag{11}$$

per mode, for real dispersion relations (i.e., propagation without damping). Accordingly these moments, like spectral moments, can serve as propagation-invariant features for classification of waves propagating in dispersive channels. However, when there is damping in addition to dispersion, these time-domain moment-like features will in fact change with propagation distance, as will the spectral moments $\langle\omega^n\rangle_x$. In the next section, we consider features that are invariant to both frequency-dependent attenuation and dispersion.

3 MOMENTS INVARIANT TO DISPERSION AND DAMPING

We consider power-law damping, wherein the attenuation (in dB) increases linearly with log-frequency, and exponential damping, wherein the attenuation (in dB) increases linearly with frequency, and give the signal processing to obtain features invariant to these damping effects, as well as dispersion (for any dispersion relation $K_r(\omega)$).

3.1 Power-law damping

Consider damping given by

$$B(x,\omega) = B(0,\omega)\,\omega^{-px}, \qquad p > 0, \tag{12}$$

which corresponds to complex dispersion with $K_i(\omega) = p\,\log(\omega)$, and results in frequency-dependent attenuation (in dB) that is linear with log-frequency. In order to extract features that are invariant to this damping, we propose the following feature extraction process. We first take the derivative of the natural logarithm of the spectral envelope,

$$Z(x,\omega) = \frac{\partial}{\partial\omega}\ln B\,(x,\omega) = \frac{B'\,(0,\omega)}{B\,(0,\omega)} - \frac{px}{\omega} \tag{13}$$

In order to eliminate the frequency-dependence of the attenuation, we now multiply by ω, to obtain

$$\omega Z(x,\omega) = \omega\frac{B'\,(0,\omega)}{B\,(0,\omega)} - px \tag{14}$$

The shape of the function $\omega Z(x,\omega)$ does not change with propagation distance x, it is merely shifted in overall level by px. By normalizing the mean of the function to zero, we eliminate the level shift. The feature function $Z_0(x,\omega)$ is defined as

$$Z_0(x,\omega) = \omega Z(x,\omega) - mean\,\{\omega Z(x,\omega)\} \tag{15}$$

where $mean\{.\}$ denotes the mean over frequency ω.

Accordingly, the spectral function $Z_0(x,\omega)$ depends only on the initial wave $u(0,t)$ and does not vary with propagation distance. Hence, features extracted from $Z_0(x,\omega)$ are, by design, independent of the propagation channel (specifically, dispersion and damping), and may serve as features to distinguish between different initial waves arising from different objects. To obtain time-domain features, we exponentiate $Z_0(x,\omega)$ and transform back to the time domain to obtain the augmented wave,

$$v(x,t) = \frac{1}{\sqrt{2\pi}}\int \exp\left(Z_0(x,\omega)\right) e^{-j\omega t}\,d\omega \tag{16}$$

Like the function $Z_0(x,\omega)$, the augmented wave $v(x,t)$ is unaffected by dispersion and damping, and depends only on the initial wave $u(0,t)$. Time-domain moment features are computed by

$$T_n(x) = \int t^n\,|v(x,t)|^2\,dt \tag{17}$$

We call the temporal moments extracted from $v(x,t)$ *attenuation and dispersion-invariant moments* (ADIMs). This feature extraction processing is illustrated in Fig. 1.

3.2 Exponential damping

Exponential frequency-dependent attenuation may be modeled as

$$B\,(x,\omega) = B\,(0,\omega)\,e^{-\beta\omega x} \tag{18}$$

which corresponds to $K_i\,(\omega) = \beta\omega$.

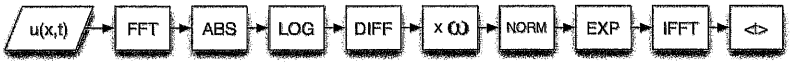

Figure 1: **Procedure for computing attenuation-and-dispersion-invariant moments for power-law damping.**

In order to extract features that are invariant to exponential damping, a process similar to that given in the previous section is used. Taking the derivative of the logarithm of the spectral envelope, we have

$$Z(x,\omega) = \frac{\partial}{\partial\omega}\ln B(x,\omega) = \frac{B'(x,\omega)}{B(x,\omega)} = \frac{B'(0,\omega)}{B(0,\omega)} - \beta x. \tag{19}$$

Observe that the spectral shape of $Z(x,\omega)$ does not change with propagation distance, but is merely shifted in overall level by βx. As in the previous section, this propagation-dependent level shift may be eliminated by normalizing the mean of the function to zero,

$$Z_0(x,\omega) = Z(x,\omega) - mean\{Z(x,\omega)\} \tag{20}$$

and then proceed as in Eqs. (16) and (17) above to obtain the temporal ADIM features. This feature extraction processing is illustrated in Fig. 2.

Figure 2: **Procedure for computing attenuation-and-dispersion-invariant moments for exponential damping.**

4 SIMULATIONS

This section describes classification simulations conducted to compare the performance of the ADIMs to that of moments invariant to dispersion only (DIMs), and to ordinary central temporal moments (MOMs), which are not invariant to either dispersion or attenuation. The simulations were conducted using numerical methods to compute the sonar backscatter from air-filled steel shells in water and the subsequent propagation of the wave through a dispersive channel model with damping (Fig. 3). Random variations in channel parameters were also investigated.

Resonance scattering theory (RST) was used to formulate the sonar backscatter for two air-filled steel shells in water, one sphere and one cylinder. [2,3,12] The number of modes used to construct the sonar backscatter for each shell was five; including higher modes did not appreciably change the waveform generated (we investigated up to 50 modes). The density and sound speed properties of the materials [4] are given in Table 1.

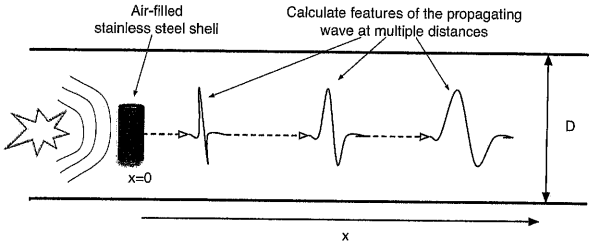

Figure 3: **Schematic overview of simulations.**

Table 1: Physical parameters used in simulations

	Water	Air	Steel
Density	$1000\frac{kg}{m^3}$	$1.2\frac{kg}{m^3}$	$7800\frac{kg}{m^3}$
Speed of Sound Waves	$1500\frac{m}{s}$	$340\frac{m}{s}$	$5880\frac{m}{s}$ (dilatational), $3140\frac{m}{s}$ (shear)

The goal was to distinguish between the sphere and cylinder using the moment features extracted from the propagated echoes. The shells were insonified by an impulsive interrogating waveform, and the backscattered pressure obtained via RST was used as the initial waveform $u(0,t)$ in the channel at position $x = 0$. This initial backscattered wave was then propagated to several distances in a channel model with dispersion relation

$$\kappa = K(\omega) = K_r(\omega) + jK_i(\omega) \tag{21}$$

where

$$K_r(\omega) = \frac{1}{c}\sqrt{\omega^2 - \left(\frac{\left(m-\frac{1}{2}\right)\pi c}{D}\right)^2} \tag{22}$$

is the dispersion relation for a two-plate waveguide [11], and $K_i(\omega)$, the damping term, is either power-law or exponential.

In the above equations, κ is the horizontal wavenumber [rad/m], ω is the frequency [rad/s], c is the sound speed in the medium [m/s], m is the propagating mode number of the waveguide, and D is the plate separation (depth of the channel [meters]). The waveform at any distance x is given by Eq. (1). Note that mode separation is implicit in our simulations, as we consider only the first propagated mode in the channel ($m = 1$ in Eq. (22)). Also note that the two-plate channel model implicitly has a low-frequency cut-off, since K_r becomes purely imaginary when $\omega < \frac{\left(m-\frac{1}{2}\right)\pi c}{D}$. Hence, frequencies below this value do not propagate in the model.

The classification features extracted from each simulated propagated echo were ordinary central temporal moments given in Eq. (9) for $n = 2, 3$, the corresponding DIMs given in Eq. (8), and the corresponding ADIMs given by the procedures discussed in Sections 3.1 and 3.2. All moments were normalized by the respective zero-order moment so that differences in signal energy between the classes would not contribute to classification performance. Receiver operating characteristic (ROC) curves were generated in order to compare classification performance of the features.

The geometry of the shells (i.e. size and thickness) were chosen to be realistic for underwater shells that might be encountered, and to be sufficiently distinguishable from the initial backscatter prior to propagation through the simulated channel. The inner and outer radii of the sphere and cylinder are given in Table 2.

Table 2: Geometry of shells used in simulations

	Inner Radius (m)	Outer Radius (m)
Sphere	0.90	1.00
Cylinder	1.38	1.40

For the simulations reported here, the depth of the channel (D) was fixed at 50 meters, with isovelocity water sound speed of $c = 1500$ m/s (mean sound speed for the case of the random channel simulations presented). Feature values were calculated at 5 meter increments starting at $x = 5$ meters, up to a maximum range of 5 kilometers. A feature vector for each moment was calculated for each shell, resulting in 12 total feature vectors. The feature values were calculated from the first propagating mode in the waveguide ($m = 1$). The sampling frequency was fixed at 10 kHz, and an anti-aliasing filter was applied to limit the bandwidth of the backscattered echoes to 5 kHz.

We first examine the case of power-law damping, which implies a dispersion relation as given in Eq. (21) with

$$K_i(\omega) = p \log(\omega). \tag{23}$$

For this simulation, $p = 5 \times 10^{-5}$. Simulated waveforms and corresponding spectrograms are shown in Figs. 4 and 5. At $x = 5$ meters (Fig. 4), the spectrograms show that most of the energy in the backscattered waveforms is concentrated in the specular impulse. As the wave propagates further through the channel (Fig. 5), the lower frequencies are increasingly delayed with respect to the higher frequencies, while the energy at higher frequencies is moderately attenuated relative to the lower frequencies.

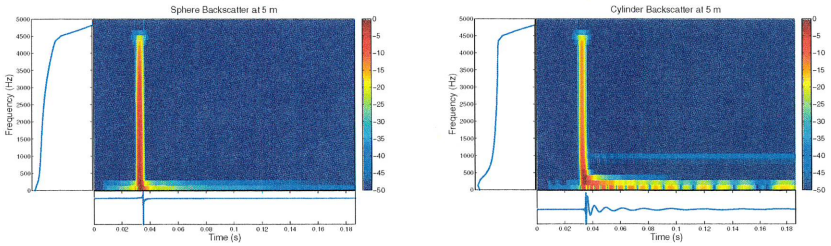

(a) (b)

Figure 4: **Spectrograms (main color panels) of backscattered echoes propagating in a channel with dispersion and damping, from the (a) sphere and (b) cylinder at $x = 5$ meters for power-law damping with $p = 10^{-5}$. The waveform is shown along the bottom of each plot, and the left panel in each plot shows the (log) spectrum.**

The classification results of this simulation ($p = 10^{-5}$) are presented in Fig. 6. For $n = 2$ and $n = 3$, the ADIMs achieve perfect classification, while the DIMs and MOMs show significantly less classification utility.

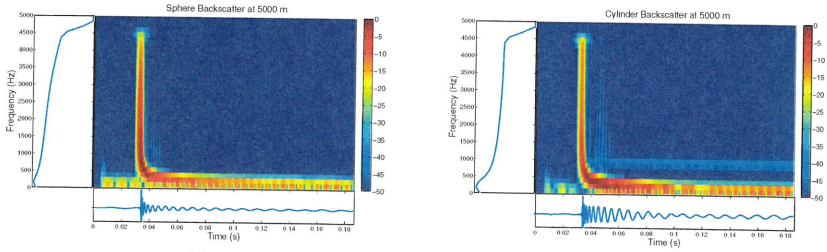

Figure 5: **Spectrograms of backscattered echoes from the (a) sphere and (b) cylinder at $x = 5000$ meters for power-law damping with $p = 10^{-5}$.**

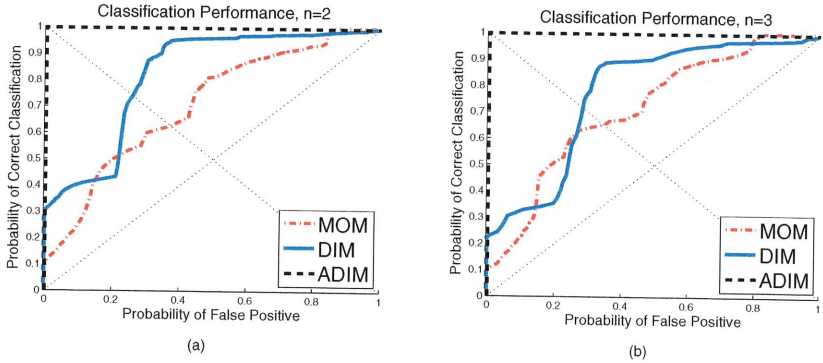

Figure 6: **ROC curves showing classification utility of ordinary temporal moments (MOM), dispersion-invariant moments (DIM), and attenuation-and-dispersion-invariant moments (ADIM) for (a) second-order moments ($n = 2$) and (b) third-order moments ($n = 3$), in a dispersive channel with power-law damping, $p = 10^{-5}$.**

We next examine the classification performance of the features in a random dispersive channel with exponential damping. The dispersion relation is given by Eq. (21) with

$$K_i(\omega) = \beta\omega. \tag{24}$$

For this simulation, two parameters governing propagation are made to be random variables, that is, at each distance a new realization is drawn and the wave at that point is calculated. The isovelocity sound speed (c) is modeled as a Gaussian random variable with mean 1500 and standard deviation 10. The attenuation factor (β) is modeled as an exponential random variable with rate parameter $\lambda = 10^8$, corresponding to a mean equal to 10^{-8} and standard deviation also equal to 10^{-8}. The classification results of this simulation are presented in Fig. 7. The ADIMs display significantly better classification utility than the DIMs or MOMs.

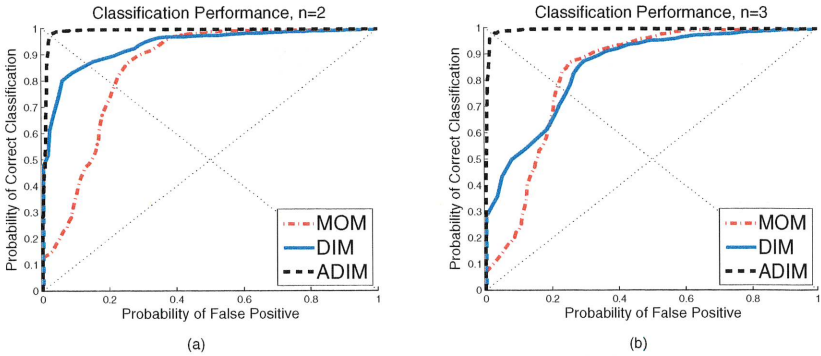

Figure 7: **ROC curves showing classification utility of ordinary temporal moments (MOM), dispersion-invariant moments (DIM), and attenuation-and-dispersion-invariant moments (ADIM) for (a) second-order moments ($n = 2$) and (b) third-order moments ($n = 3$), in a random dispersive channel with exponential damping.**

5 CONCLUSION

A propagating sonar signal can undergo frequency-dependent propagation effects such as dispersion and damping, which can be especially significant in shallow water channels. These effects are detrimental to classification performance, because differences between received echoes may reflect propagation effects rather than two different sources (targets). We presented feature extraction processing algorithms aimed at achieving propagation-invariant classification of sonar echoes in channels with dispersion and damping. Simulations were performed to examine the classification utility of the "attenuation and dispersion invariant moment" (ADIM) features, compared to ordinary central temporal moments, as well as our previously-defined dispersion-invariant moments. Random variations in channel properties were also investigated via simulations. The results demonstrated the superior classification utility of the ADIMs compared to the other features. Mode separation was implicit in our simulations, and is necessary in general to achieve the invariant classification performance of the ADIMs. While performance of the ADIMs (as well as that of ordinary moments) will degrade in the presence of multiple channel modes, preliminary investigations suggest that the ADIMs still have greater classification utility than ordinary moments; further research into this issue is ongoing.

References

[1] L. Cohen and P. Loughlin, "Dispersion – its effects and compensation," in F. Sadjadi (ed.), *Physics of Automatic Target Recognition*, Springer, 2007.

[2] G. Gaunaurd and D. Brill, "Acoustic spectrogram and complex-frequency poles of a resonantly excited elastic tube,"*J. Acoustic. Soc. Am.*, vol. 75, no. 6, pp. 1680-1693, 1984.

[3] G. Gaunaurd and W. Wertman, "Transient Acoustic Scattering By Fluid-loaded Elastic Shells,"*Int. J. Solids Structures*, vol. 27, no. 6, pp. 699-711, 1991.

[4] G. Gaunaurd and H. Strifors, "Frequency- and Time-Domain Analysis of the Transient Resonance Scattering Resulting from the Interaction of a Sound Pulse with Submerged Elastic Shells," *IEEE Trans. on Ultrasonics, Ferroelectrics, and Frequency Control*, vol. 40, no. 4, pp. 313-224, 1993.

[5] P. Loughlin and L. Cohen, "Moment features invariant to dispersion" *Proc. SPIE Defense & Security Symp., Automatic Target Recognition XIV*, vol. 5426, pp. 234-246, 2004.

[6] P. Loughlin and L. Cohen, "Phase-space Approach to Wave Propagation with Dispersion and Damping," *Proc SPIE Vol. 5559, Advanced Signal Processing Algorithms, Architectures, and Implementations XIV*, Oct 2004.

[7] P. Loughlin and L. Cohen, "Wigner distribution approximation for wave propagation," *J. Acoust. Soc. Amer.*, vol. 118, no. 3, pp. 1268-1271, 2005.

[8] G. Okopal, P. Loughlin, and L. Cohen, "Recognition of Propagating Vibrations and Invariant Features for Classification," *Proc SPIE Vol. 6234, Automatic Target Recognition XVI*, May 2006.

[9] H. C. Strifors, G. Gaunaurd, and A. Sullivan, "Reception and Processing of Electromagnetic Pulses After Propagation Through Dispersive and Dissipative Media." *Proc SPIE Vol. 5094, Automatic Target Recognition XIII*, Sep 2003.

[10] H. C. Strifors, *et. al.* "A Method for Classifying Underground Targets and Simultaneously Estimating Their Burial Conditions." *Proc. SPIE Vol. 5807, Automatic Target Recognition XV*, May 2005.

[11] I. Tolstoy and C. S. Clay,*Ocean Acoustics: Theory and Experiment in Underwater Sound*, Acoustical Society of America, 1966.

[12] C. Tsui, G. Reid, and G. Gaunaurd, "Resonance scattering by elastic cylinders and their experimental verification,"*J. Acoust. Soc. Am.*, vol. 80, no. 2, pp. 382-390, 1986.

[13] G. B. Whitham, *Linear and Nonlinear Waves*, Wiley, 1974.